COOLING RATE OPTIMIZATION OF AS-CAST CONSCIOUSLY CAST STEEL

M. R. Allazadeh

* *mrallazadeh@yahoo.com*
Received: January 2012   **Accepted: August 2012**

University of Pittsburgh, Mechanical Engineering Department, Pittsburgh PA, 15261·

Abstract: *Combination of a finite element method (FEM) algorithm with ANSYS codes and post image processing of NDT ultrasonic images along with laboratory cooling experiments and microstructural analysis provides a guideline to determine the optimum cooling rate for any grade of steel in which the highest productivity can be achieved without any degradation of the cast steel products. The suggested FEM algorithm with ANSYS codes is introduced to develop a quasi real models to simulate quenching of as-cast steel with any cooling rate from any initial temperature below steel's melting point. The algorithm builds a model which is capable to approximate the thermodynamic stresses generated by thermal strain and possible solid-solid phase transformation for as-cast steel with any chemical composition. The model is applicable for any casting geometry (slab, billet and bloom, bar, etc.) and adaptable for any method of cooling (unidirectional or multidirectional). Cooling with any cooling agent can be simulated with the algorithm in an ideal case. The phase transformation of the steel in the algorithm can be controlled by Continuous Cooling Transformation (CCT) Diagram obtained from analytical calculation or real time-temperature-transformation experiments for the cast steel. A function for optimizing cooling rate is suggested.*

Keywords: *Cooling rate, Optimization of production rate, Cast steel, continually casting steel, FEM algorithm, ANSYS*

1. INTRODUCTION

One of the challenging subjects in the steel production industry has been optimizing the cooling rate of quenching as-cast steel to room temperature to have higher productivity without lowering the quality of the cast steel. When steel cools from a high temperature, residual stresses are developed due to thermal, mechanical or transforming austenite to other phase configurations. The products of the phase transformation depend on the austenite composition and cooling rate. Stresses developed during quenching of as cast steel can raise from different sources such as, thermal stresses, volumetric stress, internal stresses, phase transformation stresses, post phase transformation stresses (interaction among the phases) and etc. These stress concentration zones are vulnerable regions to the formation of microcracks or growth of the flaws in these regions. Qualitative information about temperature evolution, cooling rate, residual stresses and distortion, assist the realistic modeling. Smolijan [1] predicted the strain and residual stress evolution within a geometrically complex specimen (e.g. cylinder, cones, spheres, etc) dealing with estimation of microstructure and hardness distribution after quenching using a mathematical method based on the finite volume method and Jominy tests results. He did not consider in his simulations any existence or formation of anomalies or defects before or after quenching. A quenching simulation for more complex geometry such as stepped cylinder and axially symmetric steel workpiece were published by other software programmers [2-3]. Chen and Meekisho [4] developed the model of a quenching process to study the effect of actual service condition aspects such as the presence of holes or notches using temperature dependent materials properties. Reti et al. [5], developed a phenomenological kinetic model flexible for both isothermal and non-isothermal conditions to describe the multiphase diffusional austenite decomposition which occurs during quenching of low alloy hypoeutectoid steel after austenization through pseudo-autonomous differential equations. Many publications are available on the simulation of the phase transitions in steel [6-14]. Some researchers implement the classical nucleation and growth theory to model the microstructure of a given austenite grain size cooling down with different rates to the ferrite- transformation temperature range [15-18]. Gur and Tekkaya [19]

combined thermal analysis and microstructural analysis with small strain elastic-plastic analysis to predict the temperature distribution, the progress of phase transformation, the evolution of internal stresses and residual stresses during quenching for axisymmetric steel components. Wang et al developed an FEM process model of quenching of steel 1080 steel cylinder in water to demonstrate austenite-pearlite and austenite-martensite transformation and suggested an elastic-plastic stress analysis [20]. Different researchers [21-25] investigated the effect of phase transformation on the residual stresses within quenched bodies. These residual stresses have an important role in changing the soundness of the steel during cooling. Nevertheless, many theoretical models were suggested to prescribe the steel quenching by researchers. Most of them, if not all, relied on the simplifications that rendered the unrealistic outcomes [1]. A wide range of cooling process analyses is based on the FEM and finite volume method (FVM) computer simulations. However, researchers [26] focused mainly on the following four basic analyses in their simulations: (a) heat transfer analysis during the cooling process (b) microstructural composition analysis via material properties, which mainly refer to thermal and mechanical properties (c) thermoplastic stress-strain analysis (d) fracture and debonding as well as void nucleation or growth analysis for computation of damage tolerance.

The objective of this paper is to introduce a method to define the optimum cooling rate for cooling continuously as-cast steel on industrial level. An FEM algorithm developed with the ANSYS codes is introduced in this research work to simulate the cooling of as-cast steel from any temperature below the solidification temperature. The algorithm is capable of being customized to simulate the thermodynamic behavior of as-cast steel microstructure with any chemical composition and any casting geometry imposed to desired cooling method. The ultimate intention of this research work is to provide a guideline on cooling process set up in continuous casting steel production for different steel compositions through NDT tests, cooling experiment tests and FEM numerical analyses. Therefore, this work will help to improve the efficiency of the casting

of steel by increasing the productivity and decreasing the inventory period of solidified continuously casting steel strand (slabs, blooms, and billets) in the production line without degrading the quality.

2. OPTIMIZATION TECHNIQUE OF THE COOLING RATE ON CONTINUOUSLY CAST STEEL PRODUCTION LINE

Solidification is a major source of creation of anomalies in the bulk material. Kianfar et al. [27] claimed to simulate three dimensional simulation of solidification in a horizontal billet continuous casting for an industrial billet caster. In addition, residual and local stresses around anomalies or in the vicinity of grain boundaries are the source of microcrack or crack propagation during heat treatment and cooling of solidified hot steel [28]. Additive elements to molten steel during continuous casting may introduce inclusions to the microstructure of the strand, which may change the defect density of the hot as-cast steel during cooling. Author has discussed the effect of the chemical composition of the inclusion on the distribution of the stress concentration zone in the steel microstruture during cooling in [29] by two dimensionless parameters. These parameters are the stress concentration factors and the inclusion rigidity factor.

Therefore, to determine the maximum cooling rate, it is essential to extract the information of the as-cast steel microstructure and defects characterizations on production line. The extracted data should include the density, size, type and location of all inclusions, voids and flaws or cracks within the as-cast steel. The ultrasonic NDT post image processing developed by author, whose detail was published in [30], coupled with the DT microstructural analysis, provides information to decode further the information embedded in the NDT tests images. In this NDT post image processing technique, a Microsoft Excel program was coupled with a commercial software ultrasonic image processing process and analyzes the NDT parameters to specify the type of the anomalies in the microstructure and the three dimensional objective Cartesian coordinate position of the

defect in the microstructure. Thereby, it can provide a three dimensional image of the microstructure of the as-cast steel after secondary cooling stage on continuously cast production line. These images are used by an FEM algorithm to approximate the stress configuration of the microstructure and predict the characteristic date of all existing anomalies after cooling hot as-cast steel to room temperature with different cooling rate. An FEM algorithm developed with the ANSYS codes introduced in this paper simulates the cooling of as-cast steel from any temperature below solidification temperature. The algorithm is capable to be customized to simulate the thermodynamic behavior of as-cast steel microstructure with any chemical composition and any casting geometry for a desired cooling method. The phase transformation simulations were based on the CCT diagram and, therefore, they were quasi-real models. The models predict, numerically, the generation of the stress concentration regions due to the thermodynamic strains during cooling a sample from the austenite temperature range with different cooling rates. The correction factors for the computation parameters and FEM variables reserved within the algorithm provide adjusting tools for different simulation case to increase the precision of the results in industry.

3. THE FEM ALGORITHM TO PREDICT STRESS DISTRIBUTION WITHIN COOLING AS-CAST STEEL

A mathematical model requires three types of formulation to simulate the cooling process of the as-cast steel with austenitic microstructure: the transformation process, cooling rate and elastic-plastic deformation within the microstructure. The simulation of a cooling process is formulated by the heat transfer governing equations defined in many academic course books. All the heat transfer mathematical models follow two main steps, first, establish a stress strain relationship based on thermodynamic constitutive laws, and, second, develop a proper method to demonstrate real heat data evolution [1]. A quasi real ANSYS program is developed to approximate the stress distribution during cooling through thickness of

cast steel with different cooling rate and defined boundary conditions the same as those imposed in the experimental process in an ideal case (no bubble formation, homogenous constant temperature, etc.). The level of complexity of the effective factor on cooling rate depends on the number of different phenomena contributing to modify the microstructure of the steel during cooling from the austenite temperature. Some of these phenomena are phase transformation, diffusion and impurity segregation, modifying the unit cell and atoms arrangement during phase transformation, localized stresses due to thermal volume changes and many other factors.

The algorithm presented in the Figure 1 computes the thermal gradient within the microstructure and thermal structural contraction resulted from temperature drop in the cooling process within the acceptable precision for defined thermal and mechanical properties of steel. Unlike most of the numerical simulations which calculate the change of phase fraction during simulation, the cooling curve-phase transformation data are based on the experimental results from CCT diagrams in the algorithm presented in Figure 1. Therefore, the numerical model introduced in this paper is quasi-real since not only the material properties, geometrical information and boundary conditions are based on the experimental model but also the decomposition of austenite into product phases of the phase transformation is read from a database provided to the program by the user. The CCT diagram furnishes this information for the model to be able to simulate the cooling of a steel slab with different cooling rates for given chemical compositions. The CCT diagram can be provided to the algorithm by commercial software such as JMATPRO whose graph is an analytical approximation or experimental results performed for a given steel grade (i.e. steel with defined chemical composition). Therefore, the model can simulate both a simple cooling curve and a complicated cooling path process for a wide range of different types of steel. Nevertheless, the priority of phase transformation is determined by the CCT diagram introduced into the program. ANSYS Parametric Design Language (APDL) is utilized to introduce the CCT diagram into the
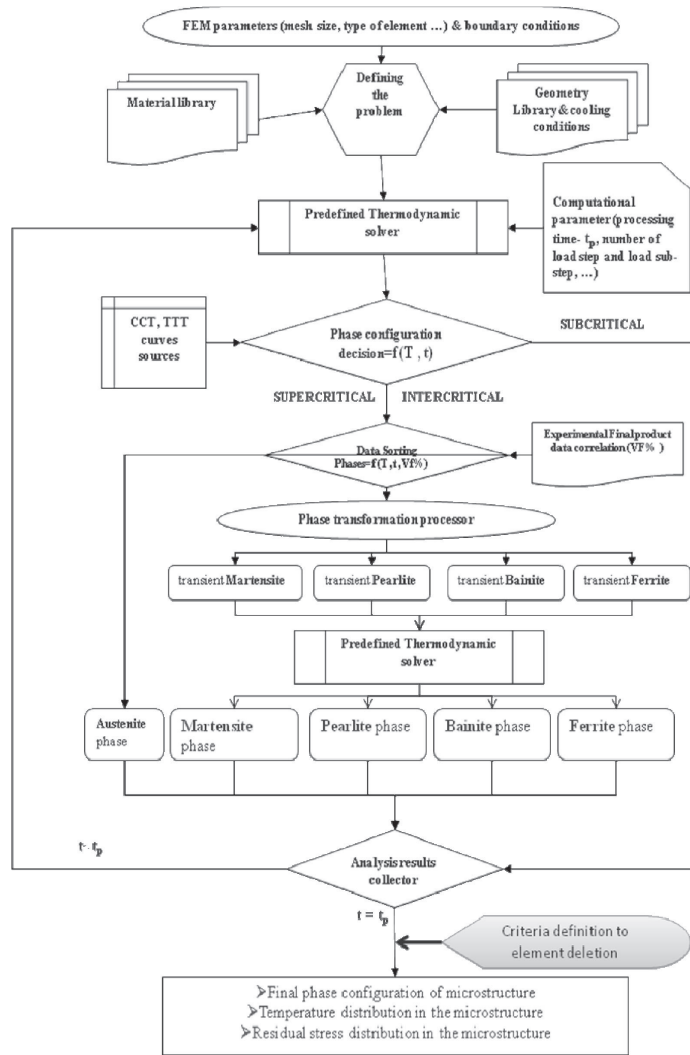
M. R. Allazadeh

Fig. 1. Flow chart of the FEM algorithm proposed to simulate cooling of as-cast steel slab.

FEM code and couple the thermal and dynamic analysis. The qualitative and quantitative information about the elements in the microstructures of each sample can give the approximate phase transformation temperature as a function of alloy content, time and temperature. The block specified for the decision of phase transformation judges the necessity of the phase transformation and furnishes the information for data sorting to introduce the phase configuration of the microstructure after each load step. The model was designed to be controlled with the volume fraction of phases presented in the final

microstructure after cooling to room temperature to increase the accuracy of the stress analysis. The volume fraction phases presented in the microstructure after transformation of austenite to the other phases follow the unity percentage rule in the algorithm as next;

$$(\%ferrite + \%pearlite + \%bainite + \%martensite + \%austenite + \%other\ phase)/100 = 1 \qquad (1)$$

The experimental kinetics of the isothermal phase transformation for ferrite, pearlite, and bainite can be calculated by Johnson-Mehl-

4

Avrami governing equation as [6-8];

$$V_k = V_y (1 - e^{-b t^n}) \qquad (2)$$

where V_k and V_y are the volume fraction before and after transformation. t is the quenching time, b and n are temperature dependent phase constants. Then Koistimen and Marburger [31] deployed the same method to define the relationship between volume fraction before (V_m) and after (V_n) the martensite transformation as shown in Equation 3;

$$V_m = V_n (1 - e^{-c(M_S - T(t))}) \qquad (3)$$

where M_s is the martensite start temperature in the CCT diagram and T(t) is the temperature of the material at given time, t. The value of the constant, c, is given in the literature as 0.011 [19]. If the final product of the cooling is known, the program can be set to mimic the experimental data for final volume fractions of different phases in the microstructure. Therefore, instead of estimating the phase fractions with Equations 2 and 3, the actual volume fracture for the phases are embedded in the program as a function of the thermal expansion coefficient. It reduces the calculation of the residual stress within the final microstructure.

The structure deformation within the element due to the solid-solid transformation carries out by introducing thermo-elastic strain into the elements subjected to the phase transformation in an isothermal condition. The nodal and element outcomes of the proposed algorithm in the ANSYS provide the final phase configuration of the microstructure and thermal distributions and accumulation stress concentration zones. Thereby, the results can mark the vulnerable region to the formation of microcracks or the growth of flaws. The models were designed for thermally induced stresses (such as those resulting from cooling) rather than mechanically applied stress models. The maximum stress concentration zone usually appears at the interface of two phases in the microstructural configuration. It was observed from the results of the numerical computation that the shape of the grains changes the distribution of stress concentration zones [28, 32]. The algorithm can simulate the cooling and solid-solid phase transformation processes for used defined grain shape. The collection of the numerical simulations, resulting from different steps of the accelerated cooling simulation, indicates that the stress concentration zones generated by solid-solid phase transformation were stored in the microstructure which some example of such numerical results will be presented in this paper. The properties of the grain boundaries (GB) play important roles in the intensity of the accumulated residual stresses during accelerated cooling of as-solidified steel. This fact can be observed in the results of the numerical simulations in the other publications [28, 32]. Four different methods are available in the developed ANSYS program to build interfacial region between grains representing GB. These four intergranular interaction methods built in the presented algorithm are;

- Interfaces formed by glued grains: ANSYS merge the nodes at contact surfaces of two adjunct grains so there is not any discontinuity for thermodynamic fields at grain boundaries by other word the grain boundary is ignored in the simulations.

- Thin layer bodies: they are built by meshing interspaces regions between adjacent grains surfaces, these elements possess complete set of thermo-dynamic material properties, this GB model can be tuned up to provide GB properties with better accuracy in compare to other GB models.

- Contact element interface method: ANSYS defined master-slave interaction among the nodes at the interfacial surfaces of the adjacent grains by giving dynamic properties to the nodes of the contact surfaces.

- Cohesive zone interface method: ANSYS generates interfacial elements with cohesion properties built by the nodes of contact surfaces of adjacent grains.

In the numerical model presented in this work, the inter-granular cracks are simulated by including the properties defined for the grain boundary of the microstructure. This increases the precision of the simulation. However, it causes discontinuity and convergence problems
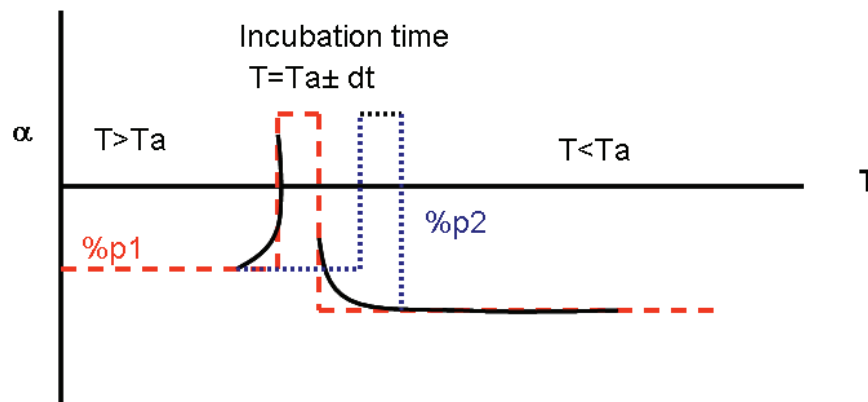
Fig. 2. Heaviside function introduced in the definition of the thermal expansion coefficient for specific steel grade to simulate the phase transformation numerically;

in the mathematical calculation in the code. Interaction of atoms and metallurgical behavior of unit cells in a crystal are more complicated than the continuum model used in the FEM simulations, many factors were also neglected in these simulations to simplify the model. However, the models are able to present the residual stress concentration within the microstructure during cooling. In the model, the heat was considered to transfer due to three modes of the heat transferring of conduction, convection and radiation. The material was assumed to be perfectly isotropic, which for multi crystal material is a reliable assumption. It is important to note that the computation time was not the same as real time in the cooling experiment. The relation between real time in the CCT diagram and computational time was set through a number of time steps per second. This value was set in a time correction factor, (TCF), whose value is a function of different factors of the steel sample microstructure. Some of these factors are steel chemical composition, size of the sample of the model, method of building grain boundaries, meshing size and type of elements used in the model as well as microstructure information such as grain size, quantity and distribution of anomalies in the microstructure and degree of homogeneity. Therefore, the value of the TCF should be set experimentally to employ the phase transformation in the model accurately. The proposed algorithm builds the model based on the chosen type of the steel composition from the material library and steel product geometry library. Then it applies the computational parameters and FEM parameters to the model.

Three types of the controls were embedded within the algorithm to adjust the precision after each time step. These thermodynamic controls are transformation control, cooling rate control and thermodynamic strain induced control. Phase transformation control mimics the behavior of the unite cells in the solid-solid phase transformation and the dynamic changes in the structural bodies by applying the phase transformation deformation on the atomic crystal cell in the meshing elements to represent the transformation of the grain phases as a result of diffusion and diffusionless atomistic movements in the steel microstructure. This crystal cell deformation was formulated in the material properties by Heaviside step function to induce the deformation of solid-solid transformation behavior of the unit cell and grain boundaries in the model.

The Heaviside function was implemented in the definition of the heat expansion coefficient. The definition of the heat expansion coefficient for each phase is based on the experimental data of the CCT diagram for a given steel composition. Figure 2 is a general definition for temperature dependent Heaviside type thermal expansion coefficient function. The algorithm utilizes the thermodynamic changes and Heaviside function during transformation of the austenite phase to the product

6

of solid-solid phase transformation via transient phase corresponding for each type of the austenite phase transformation. The transient phase performs the changes in the size of the unit cells in the isothermal condition. The cooling curve in the quasi-real mathematical models given in the algorithm is calculated by a linear function defined between the range of the temperatures known for a given phase fraction. It can also be noticed in Figure 2 that the isothermal solid-solid phase transformation is considered over a small temperature range rather than at critical temperature. This is required for the convergence condition of the program which results in an ill-function of the equation and it also is a requirement for the incubation time of the transformation.

The desired cooling rate is adjusted with cooling rate control designed in the suggested FEM algorithm: A more efficient solution of controlling the cooling rate is to introduce the cooling rate via the behavior of the thermal properties of the material. A material control rate of heat flux is proposed in the algorithm based on the classical conductivity equation. Thermodynamic strain induced control was inserted in the FEM algorithm to monitor the strains generated during the cooling process of the as-cast steel. Cooling steel slabs from the austenite temperature range, creates both strain induced due to thermodynamic effects on the microstructure and solid to solid phase transformation phenomena resulting from formation of other phases (ferrite, bainite, martensite,….) out of the austenite phase. The strain developed in the microstructure may result in increasing the density of cracks and flaws in which they are modeled by fracture constitutive laws. The thermal induced strain exists because of the heat flux out of the body during quenching and it calculated as a function of secant coefficient of the thermal expansion, as below [33];

$$\alpha^{Sec}(T_n) = \frac{\int_{T_O}^{T_n} \alpha^{ins}(T)dT}{(T_n - T_{Ref})} \quad (4)$$

where T_o and T_n are temperatures at which α^{sec} is evaluated and defined, respectively. T_{ref} is the zero thermal strain temperature which in most

cases in the calculation is equal to T_o. This variation in the coefficient of thermal expansion is defined by defined temperature at critical points of the Heaviside function. ANSYS defined the values between the defined temperature by a linear function and constant for the temperature below and above the defined temperature range in the table by extreme points of minimum and maximum temperature in the data table, respectively.

4. VALIDATION OF THE FINITE ELEMENT MODEL

The ANSYS meshing element designated as plane 223 was used for the thermo-elastic analysis during cooling. The plane 223 element has eight nodes with up to four degrees of freedom per node and capability of coupling fields.

To verify the cooling process of the FEM model experimentally under laboratory conditions, a block of 75 x 75 x 50 millimeters from the continuous cast steel slab AISI-1010 was cut. The sample was verified by the pretest ultrasonic NDT images to be nearly anomaly-free. The NDT method and results were explained in detail in [30]. To monitor the temperature variation through the sample thickness during cooling experiments, all samples are drilled with a 3 mm drill bit, almost twice the diameter of the thermocouple, to avoid sticking the thermocouple inside the hole because of volume changes due to high temperature during heat treatment. The holes were drilled at 6.25, 12.5 and 25 millimeters from the top surface (cut surface from the slab), at midsection of the sample. Figure 3 shows the dimensions of the samples used for this experiment. The furnace was set to the austenite temperature range between 900 °C -1100 °C and was kept for 15 to 30 minutes at this temperature to eliminate the temperature gradient across the furnace before putting the specimen inside the furnace. A three channel Lab view interface program recorded the data from the sample in real time. The program presented the data in both real time and average over 50 points' samples data in two different graphs as the experiment proceeded. The

program is set with data acquisition (DAQ) rate of 1000 Hz, effective DAQ 20 sample/second. The Lab view program runs in a desktop PC computer and DAQ channels were connected to three thermocouples, which were inserted into the sample holes. The sample is put in and out of the furnace using tongs. A conveyer facilitated smooth sliding of the sample between the oven and the quenching table to avoid removing the thermocouple from its place and to ensure the continuous contact of the thermocouple with the sample during the experiment. The furnace was adjusted to the desired temperature. Figure 4 is the picture of the system set up used in the experiment. Both heating and cooling processes of the steel samples needed predefined data and procedures. The purpose of the heating process in this experiment was to obtain the austenite phase. During austenization, the samples were heated above the austenite temperature and the cooling rate was monitored from the austenite phase. The start and the end range of the solid-solid phase transformation in the experiment, which was the temperature range falling between A1 and A3 in the Fe-FeC phase diagram, was estimated by JMATPRO. Data were set to be stored in real time in Excel files during the heating and cooling processes for post processing and analyzing. Before putting the samples in the furnace, the thermocouples were placed in the holes inside the sample and fixed on the sample. The tested sample was kept for two hours at this temperature according to ASTM standards to have a uniform temperature all over the specimen. The cooling rate recording was stopped near ambient
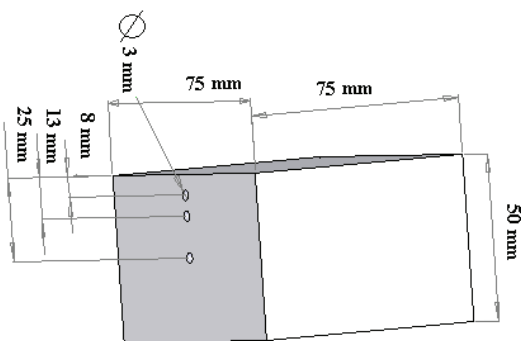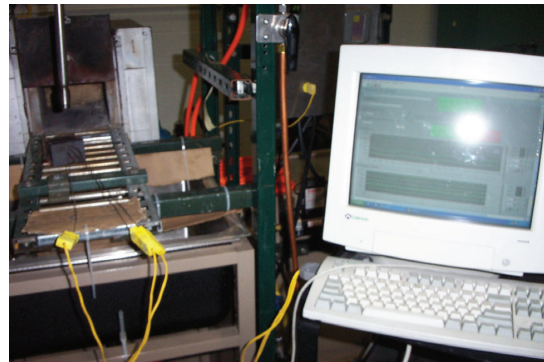

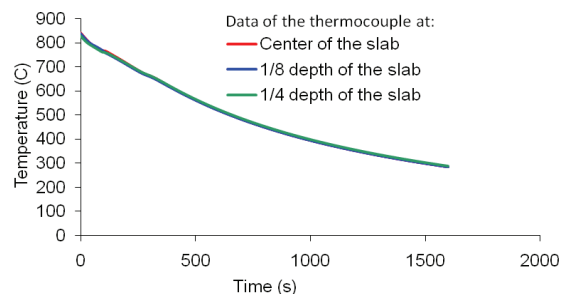**Fig. 4.** Experimental set up.

Fig. 5. Cooling rate graph related to air cooling of Steel 1010.

temperature. The experiment is the cold charging of the slab into the hot furnace and holding the slab until the microstructure has only austenite phase. The cooling rate at the first 1500 s portion of the cooling process can be observed in Figure 5. The through-thickness cooling rate from the surface to the center plane is shown in Figure 5 at four checking point cooling from 900 °C to near 100 °C by ambient temperature air. The checkpoints are measured from the top surface of the sample at quarter, middle and center planes. The cooling rate at these check points shows, as it was expected, the slowest cooling rate belongs to the center plane while the surface has the fastest cooling rate and is decreasing from surface to the center plane.

The FEM program was used to model the 1010 steel AISI grade to simulate the cooling process analytically with the sample size similar to the one used in the laboratory cooling experiment.
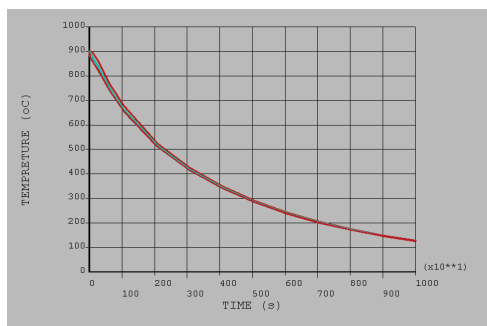

Fig. 3. Schematic view of the sample used for the cooling rate experiment;

8

Fig. 6. through thickness cooling rate of sample 1010 in the cooling model of the sample at middle section of the slab, ¼ and 1/8 depth measured from top surface.
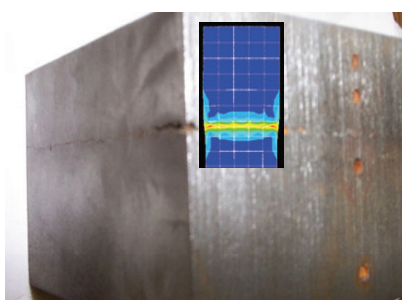

Fig. 7. Comparison of the defect formation in the laboratory cooing test sample with the result of the model simulated by the proposed algorithm.

The film or convection coefficient in the model was 25 Wm^{-2}K^{-1} [34], which is the same as air-cooling. Figure 6 is the cooling curve of the model at the middle plane based on the FEM numerical calculation. The cooling rate in Figure 5 is almost 0.4 C/s but in Figure 6 is about 1 C/s, however, both curves show same behavior. Applying a constant factor to shift the curve in Figure 6 over Figure 5 shows the correlation between numerical results computed by FEM and experimental results obtained during the cooling experiment. It is important to note no curve fitting has been deployed in Figures 5 and 6; therefore, the comparison is a legitimate verification of the cooling model and the program can be used for modeling the cooling process. It is only comparison between a continuum numerical model and experimental results to verify the thermodynamic calculation of the algorithm and the algorithm ignores some of the detail of microstructural events taken place during the experiments such as grain coarsening.

A more complicated simulation was modeled to show the stress accumulation due to strain introduced to the microstructure using the proposed algorithm in Figure 1. Then the results were compared with the crack formation in the steel grade 1010 in the described laboratory cooling test. It can be seen from Figure 7 that the stress concentration plane is the more vulnerable plate within the sample for the formation of the defect. Figure 7 is the evidence that the proposed algorithm can predict the stress concentration zone imposed to the steel microstructure by the stress generating sources and, consequently, it can give valuable information about the location of the formation of the defect, if the input information and adjusting correction factors are defined accurately.

5. OPTIMIZATION OF THE COOLING RATE USING THE SUGGESTED NUMERICAL ALGORITHM

A series of simulations designed to investigate the relationship between the residual stresses developed within the microstructure with phase configuration of the cast steel. In the models, the phase transformation of the steel is based on the CCT diagram suggested by JMATPRO for average grain size of 1000 ;m for the steel with chemical composition in Table 1, quenched with different cooling rates from 1200 °C.

The heat is transferred from the top surface of a 2-dimensional model with no heat exchange from other surfaces with the environment (i.e. adiabatic thermal conditions). Cooling rate can be controlled with three different methods as: the applied convection film coefficient, environment temperature and time parameters of the FEM computation. In these simulations, in order to have better control over changing the rate of cooling, the latter method was used. The model is constrained from the bottom. It is to simulate the half section of a 30 mm thick slab, using symmetric conditions, cooling using cooling agents from top and bottom surfaces in an ideal case (no bubble formation, homogenous constant temperature, etc.). The boundary conditions applied to the models are shown in the Figure 8.

**Table 1.** Chemical composition of steel grade 1010 used in the FEM simulations.

Element	%	Element	%	Element	%	Element	%
C	0.114	Cu	0.005	Nb	0.001	N	0.0042
Mn	0.489	Ni	0.003	Sn	0.001	As	5 e-4
P	0.009	Cr	0.005	Al-total	0.0329	Ti	0.0007
S	0.0039	V	0.001	Al-soluble	0.0303	B	1e-4
Si	0.041	Mo	0.001	Ca	0.0025	Si	0.041
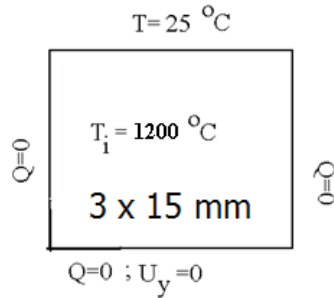
Fig. 8. Boundary conditions of the models used for studying the stress accumulation at the interface.

The material properties of all phase products formed after cooling the steel model were obtained from JMATPRO. The film or convection coefficient in the model was 500 $Wm^{-2}K^{-1}$. The emmisitivity coefficient is considered to be 0.8 for reddish to grey color of the sample from 1200 °C to room temperature. The grains are represented by body entity in the models and elements within the body are unit cells in the grains. The grain diameters are considered to be 1000 μm in the

model. The grains are homogenous and isotropic without any dislocations or any type of anomalies. The interaction between contact grains is a contact problem and, like all other contact problems, is highly nonlinear and requires significant computer resources to resolve. The solution may converge after a number of iterations or totally diverge or contact surfaces may overlap each other in a largely unpredictable and abrupt manner, depending on the loads, material, boundary conditions, and other factors [35]. The grain boundaries were defined as atoms in non-lattice sites. In this model, the grain boundaries were built with thin layer bodies' method. The material properties defined for the grain boundaries in the model are close to the material properties of the phases of adjacent grains before and after phase transformation.

Figure 9 is a summary of a series of the simulation with different time computational parameters, to impose different cooling rates. The strain induced by the austenite to martensite transformation was considered slightly smaller than the strain induced by the austenite to ferrite phase transformation. This fact was applied in the
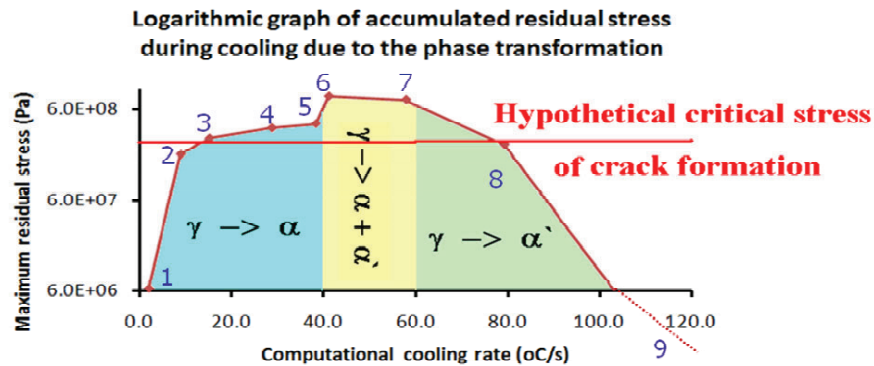
Fig. 9. Variation in the stress accumulation at the grain boundary interface due to application of different cooling rates after completion of the solid-solid phase transformation.
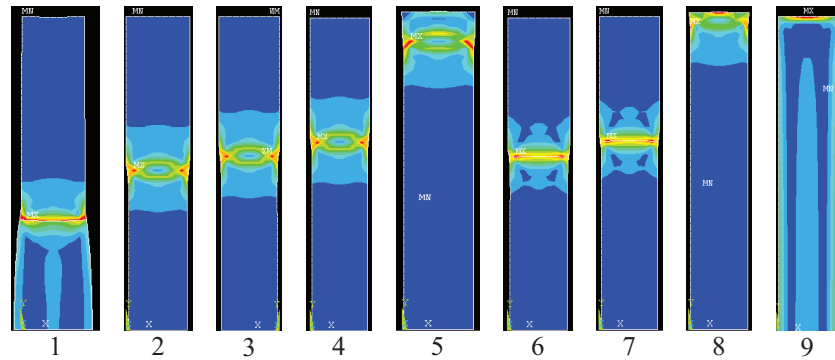
Fig. 10. Stress distributions for results of the graph in the Figure 9.
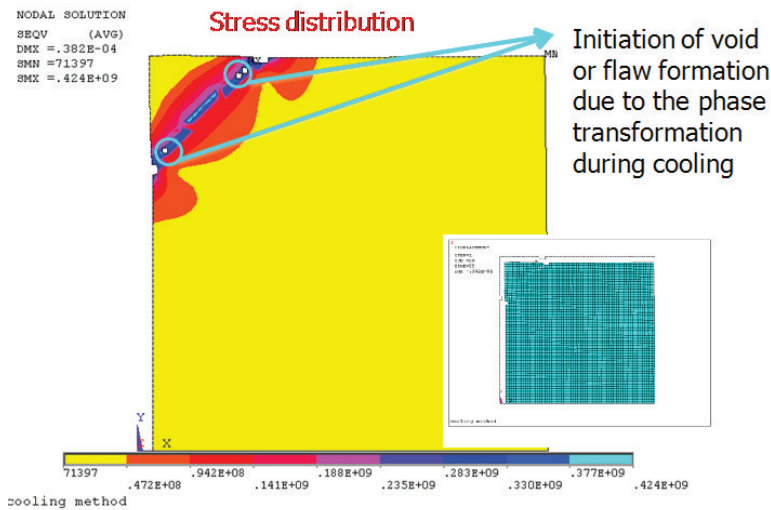

Fig. 11. Presentation of the void and initiation of flaw formation using the deletion element block in the algorithm.

algorithm based on the equation developed by Onink et al. [36] and Lee et al. [37] formulation.

The first section in Figure 9 is the austenite to ferrite transformation and it shows that the residual stress accumulation is increasing as the cooling rate accelerated. However, a slight decline in the stress accumulation can be observed in the two phase formation as the martensite formation took place with higher cooling rates. This can be a direct result of the lower strain of the martensite formation compared to the ferrite formation. The decrease of the maximum stress concentration in the third section is due to the effect of the time parameter in transforming the austenite to its solid-solid phase transformation products. The results in Figure 10 were collected after completion of the phase transformation. It can be understood by investigating the gradual transformation images in Figure 10 that in the case of a higher cooling rate the high stress concentration band is closer to the top surface and the chance for relaxation is higher. When the phase transformation is completed before the end of the load step, the additive residual stresses to the microstructure are only the result of the thermodynamic strains without influence of the phase transformation strains. It shows the importance of applying TCF parameters to assure accuracy of the results for simulation to obtain the optimum cooling rate.

The last block in the proposed algorithm in Figure 1 is to present the void and flaw initiation in the final results. If this block is placed in the time process cycle, the accuracy could be increased. However, the probability of the divergent solution and crash of the simulation gets higher as mentioned before. Figure 11 is an example of the simulation of a model with element deletion block in the algorithm. It presents the void and flaw initiation in the model. The image on the bottom right side of the Figure 2 shows that the final product of the phase transformation is martensite. In this model, the cooling was applied from the top and the left side surfaces.

The models presented in this research work demonstrated the potential concentration of residual stresses around two phase material such as iron-carbon alloys produced from solid-solid phase transformation and, on a smaller scale, due to the thermal gradient within the microstructure developed by the cooling process (e.g. around inclusions in the results presented in [29]).

The algorithm in Figure 1was used to simulate many models with focus on influence of different parameter on cooling rate. Some of these simulations can be found in previous publications of the author [28, 32]. From different simulations using the suggested algorithm, it could be concluded that the critical cooling rate depends on the following,

- Cleanliness of the microstructure (pre-existing flaws and voids),
- Initial stress state of the microstructure (σ_i),
- Chemical composition of the steel ($c\%$),
- Thermodynamic material properties of each phases,
- Microstructural configuration (single phase or multi phase),
- Grain size and grain shape (D^c_γ),
- Size of the slabs (V_s),
- Cooling procedure $(T_{s\ i=1,...,n}(\dot{T}^c_{s\ i=1,...,n}))$,
- Shape of the slabs,
- Initial temperature of the as-cast slab at the start of the accelerated cooling process (T_t),
- Grain boundary properties (σ_{coh})

To obtain a critical cooling rate, the above factors can be formulated in a cooling rate equation as:

$$\dot{T}^c_{crack\ formation} = f(T_{s\ i=1,...,n}(\dot{T}^c_{s\ i=1,...,n}), c\%,$$

$$D^c_\gamma(T^c), \sigma_{coh}, \sigma_i, T_t, \alpha_{thermal}, V_s) \qquad (5)$$

The information about the cleanliness of the microstructure on production line can be extracted from the developed NDT test published in [29]. Analytical formula embedded within JMATPRO gives the thermodynamic material properties. The rest of the parameters depend on the designed casting production line and desired cast product. The proposed algorithm can be used with different models to study different aspects of continuum behavior of microstruture during cooling process.

6. CONCLUTIONS

The main goal of this paper was to introduce a fingerprint guideline to optimize the cooling rate of continually cast steel as casting is in progress on production line. This increase the productivity of the casting line, reduce the cost of the product and increase the quality of the cast steel. The guideline suggested for this purpose includes,

- Microstructural analysis using different optical observation and investigation of the anomalies in the microstructure
- NDT tests and developed post image processing developed for this guideline,
- Laboratory data of CCT diagram for the cast steel on production line,
- Experimental results (cooling experiments, thermal expansion determination,…) to determine thermodynamic material properties of the steel with the same chemical composition as the cast steel
- The developed algorithm for the FEM program.

The algorithm could be used to study the factors influence the optimum cooling rate for quenching as-cast continuously cast steel. A function to optimize cooling rate was suggested based on the simulations generated by the FEM algorithm introduced in this paper. The steel making industries can use this fingerprints as a guide line to predict the following
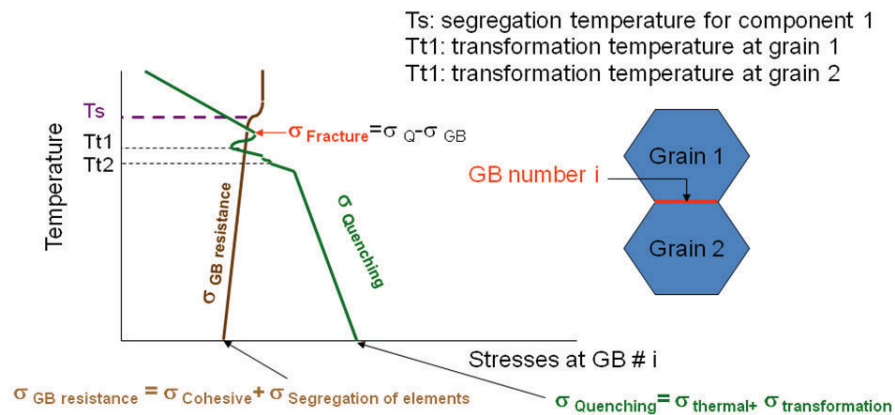
- The possibility of crack formation or

Fig. 12. Increasing the accuracy of the algorithm by including the effect of segregation elements at the grain boundary to the flaw formation.
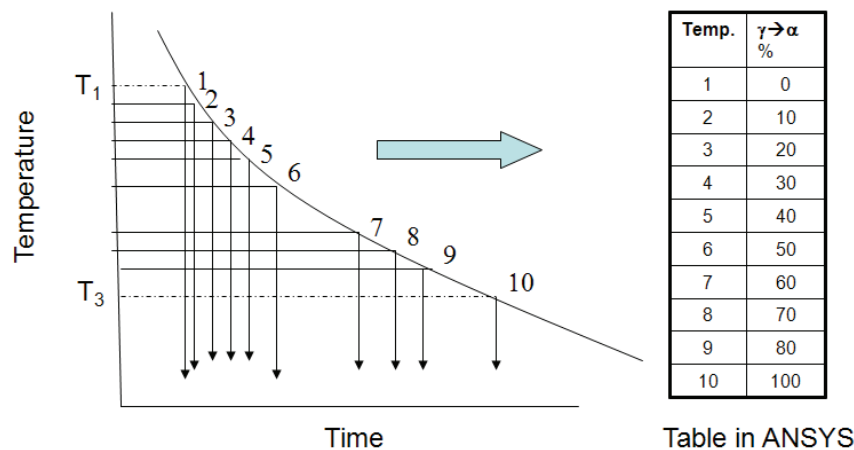

Fig. 13. Encapsulating method applied to determine the phase transformation product for each cooling rate.

propagation for the applied cooling rate,

- Information about the size of the crack for the applied cooling rate,
- A platform to investigate the relationship between the crack formation and the steel composition for a given cooling rate.
- Connection between CCT diagram and altering the defect density for a given steel composition,
- The residual stress distribution within the known microstructural configuration,

The accuracy of the steps proposed in the suggested guidelines can be increased if different advanced steps are added to it. For example, in this work, the criteria to present the flaw

initiation was based on having quenching stress higher than a constant critical value considered as cohesive stress at the grain boundary. However, the adhesion force at grain boundary varies for different steel chemical composition by the segregation of different alloying elements or the grain boundary resistance to flaw formation. Figure 12 shows that competition between tensile residual stress and grain boundary resistance to the formation of flaw as a function of segregation, determines the critical optimum cooling rate for specific grade of steel.

The correction factors in the algorithm control the accuracy of the results. The precise value of these correction factors must be obtained for each
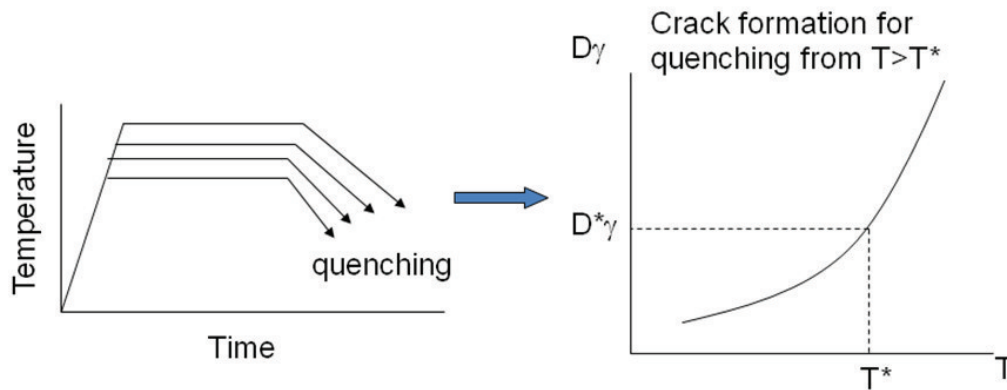
13

Fig. 14. Collecting the cooling and casting experimental data to determine the critical values of the factors influence the optimum cooling rate of the continuous casting steel for each chemical composition f the steel.

case of the cast steel via cooling experiments in the laboratory and on industrial scales. Arranging a set of encapsulating steel sample to be used in the cooling tests with different cooling rates provides the samples for microstructural investigation to determine the formation of the defect and volume fraction of the phases produced in the microstructure. Laboratory casting of steel with different compositions can regulate the correction factors designed in the algorithm to increase the accuracy of the results for the prediction of the crack formation in the continuously cast steel. Figure 13 and Figure 14 suggest these laboratories experiments which enhance the accuracy of the algorithm.

The growing demand for new steel products and competition to produce steel with higher quality and optimum production rate, will keep this research field open for many new ideas and researchers.

REFERENCES

1.	Smoljan B.; "Numerical Simulation of Steel Quenching"; ASM International, JMEPEG Volume 11(1) February 2002 11:75-79.
2.	Ehlers M., Muller H., Lohe D.; "Simulation of steel hardening"; 11th Congress of the International Federation for Heat Treatment and Surface Engineering and the 4th ASM Heat Treatment and Surface Engineering Conference in Europe; Florence; Italy; 19-21 Oct. 1998. pp. 263-272. 1998.
3.	Smoljan B., Liscic B.; "Computer simulation of quenching of steel workpieces with complex shape"; Hungarian Scientific Society of Mechanical Engineering, Heat Treatment and Surface Engineering of Light Alloys: Proceedings of the 7th International Seminar of IFHT (Hungary), pp. 339-342, Sept. 1999; 1999.
4.	Chen X. L., Meekisho L.; "Computer simulation of temperature and thermal stress fields during quenching process"; Second International Conference on Quenching and the Control of Distortion; Cleveland, Ohio; USA; 4-7 Nov. 1996. pp. 241-247. 1996.
5.	Reti T., Fried Z., Felde I.; "Computer simulation of steel quenching process using a multi-phase transformation model"; Computational Materials Science, Volume 22, Issues 3-4 , December 2001, pp: 261-278.
6.	Hougardy, H. P., Yamazaki, K., An improved calculation of the transformation of steels, Steel Res., 57 (1986), 466-471.
7.	Homberg, D., "A mathematical model for the phase transitions in eutectoid carbon steel," IMA J. Appl. Math., 54 (1995), 31-57.
8.	Homberg, D., "Irreversible phase transitions in steel," WIAS Preprint No. 131, 1994.
9.	Agarwal, P. K., Brimacombe, J. K., "Mathematical Model of Heat Flow and Austenite-Pearlite Transformation in Eutectoid Carbon Steel Rods for Wire," Metall. Trans. B, 12 (1981), 121-133.
10.	Buza, G., Hougardy, H. P., Gergely, M.,

14

"Calculation of the isothermal transformation diagram from measurements with continuous cooling, Steel Res.," 57 (1986), 650-653.

11. Hawbolt, E. B., Chau, B., Brimacombe, J. K., "Kinetics of Austenite-Pearlite Transformation in Eutectoid Carbon Steel," Metall. Trans. A, 14 (1983), 1803-1815.

12. Hengerer, F., Strassle, B., Bremi, P., Berechnung der Abkuhlvorgange beim Ol{ und Luftharten zylinder- und plattenformiger Werkstucke aus legiertem Vergutungsstahl mit Hilfe einer elektronischen Rechenanlage, Stahl u. Eisen 89 (1969), 641-654.

13. Esmailian, M.; "The effect of cooling rate and austenite grain size on the austenite to ferrite transformation temperature and different ferrite morphologies in microalloyed steels"; IJMSE. 2010; 7 (1) :7-14.

14. Poladi, A., Zandrahimi, M., "Phase Transformation During Wear of AISI Stainless Steel 316. IJMSE. 2008; 5 (3) :43-48.

15. Parker, K. V.; "Modeling of phase transformations in hot rolled steels"; PhD thesis, University of Cambridge, UK, 1997.

16. Jones, S. J., Bhadhesia, H. K. D. H.; Acta. Metall., 1997, 45(7), 2911-2820.

17. Jones, S. J.; "Modeling inclusion potency and simultaneous transformation kinetics in steels"; PhD thesis, University of Cambridge, UK, 1996.

18. Ichikawa, K., Bhadhesia, H. K. D. H.; "Mathematical modeling of weld phenomena 4"; 302-320, 1998, London, The Institute of Materials.

19. Gur, C. H., Tekkaya, A. E.; "Finite element simulation of quench hardening"; Steel research (Steel res.) ISSN 0177-4832 CODEN STLRCX , 1996, vol. 67, no. 7, pp. 298-306 .

20. Wang, K. F., Chanderansekar, R. S., Yang, H. T. Y.; "Experimental and computational study of the quenching of carbon steel"; Journal of manufacturing science and engineering (J. manuf. sci. eng.) ISSN 1087-1357, 1997, vol. 119, no3, pp. 257-265.

21. Yu, H. J.; Brechnung von Abkuhlungs, Umwandlungs, Schqweib, sowie Verformungseignspannungen mit Hilfe der Methode der Finiten Elenmente, Karlsruhe 1977,(Dr, -ing, thesis)

22. Hildenqall, B.; "Prediction of the residual stresses created during quenching"; Linkoping, 1979, (PhD thesis).

23. Sjostrom, S, Mater. Sci. Technol., 1985, pp:823-829.

24. Denis, S., Gautier, S., Simon, A., Beck, G.; Mater. Sci. Technol., 1985, pp:805-814.

25. Leblond, j. B., Mottet, G, Devaux, J. C., ; Mater. Sci. Technol., 1985, pp:815-822.

26. Liscic´, B. Tensi, H., Luty, W.; "Theory and Technology of Quenching"; ed., Springer-Verlag, 1992.

27. Kianfar, S., Seyedein, S. H., Aboutalebi, M. R., "Solidification Modeling and Dendrite Structure Analysis in a Horizontal Continuously Cast Brass Billet." IJMSE. 2008; 5 (4) :16-24

28. Allazadeh, M. R.,"The Effect of Cooling Rate on the Microstructure Configuration of Continuously Cast Steel Slabs"; dissertation thesis, 2009, University of Pittsburgh.

29. Allazadeh, M. R., Garcia, C. I., DeArdo, A. J. and Lovell, M. R., "Analysis of Stress Concentration around Inclusions due to Thermally Induced Strain to the Steel Matrix"; Journal of ASTM International, vol 6, No. 5.(2009).

30. Allazadeh, M. R., Garcia, C. I., Alderson, K. J., DeArdo, A. J.; "Using NDT Image Processing Analysis to Study the Soundness and Cleanliness of Accelerated Cooled Continuously Cast Steel Slabs"; Materials Science & Technology 2008 Conference, pages 1853-1864

31. Koistinen, D. P., Marburguer, R. E.; Acta Metall. 7, 1959, pp:59-61.

32. Allazadeh, M. R., "New FEM technique to study residual stresses developed in continuously cast steel during solid-solid phase transformation" submitted paper to Journal of Constructional Steel Research, Ref. No.: JCSR-D-10-00089 (2010).

33. Release 11.0 Documentation for ANSYS.

34. Andrezejewski, P, Drastik, A, Kohler, K U, Pluschkell W 1990 New aspects of oscillation mode operation and results in slab casting. Process Tech. Conference Proc. (Warrendale, PA: Iron & Steel Soc.) vol. 9, pp 173-181.

35. Hu, S. Y., Ludwig, M., Kizler, P. and

Schmauder, S. 1998 Atomistic simulations of deformation and fracture of alpha-Fe Modelling Simul. Mater. Sci. Eng. 6 567.

36. Onink, M., Brakman, S. M., Tichelaar, F. D., Mittemeijer, E. J., Van der Zwag, S.; Scripta Mater. 1993, 29:1011.

37. Lee, S. J., Lusk, M. T., Lee, K. Y.; "Conversional model of transformation strain to phase fraction in low alloy steels"; Acta Materalia, 55, (2007), 875-882.